LETTERS

The purpose of this Letters section is to provide rapid dissemination of important new results in the fields regularly covered by Physics of Plasmas. Results of extended research should not be presented as a series of letters in place of comprehensive articles. Letters cannot exceed four printed pages in length, including space allowed for title, figures, tables, references and an abstract limited to about 100 words. ***There is a three-month time limit, from date of receipt to acceptance, for processing Letter manuscripts. Authors must also submit a brief statement justifying rapid publication in the Letters section.***

Radial and zonal modes in hyperfine-scale stellarator turbulence

F. Jenko and A. Kendl
Max-Planck-Institut für Plasmaphysik, EURATOM Association, Boltzmannstr. 2, 85748 Garching, Germany

(Received 7 June 2002; accepted 23 July 2002)

Electromagnetic plasma turbulence at hyperfine (i.e., electron gyroradius) scales is studied in the geometry of an advanced stellarator fusion experiment, Wendelstein 7-AS [H. Renner, Plasma Phys. Controlled Fusion **31**, 1579 (1989)], by means of nonlinear gyrokinetic simulations. It is demonstrated that high-amplitude radial streamers may also exist in non-tokamak devices, raising the electron heat flux to experimentally relevant values. Moreover, some statistical characteristics of the fully developed turbulence are computed, highlighting the (co-)existence, nature, and role of self-generated zonal flows and fields. © *2002 American Institute of Physics.*
[DOI: 10.1063/1.1507591]

In contrast to the axisymmetric case of a tokamak, the magnetic field configuration of a stellarator is characterized by greater complexity and higher dimensionality. This may have important consequences for the linear and nonlinear properties of microinstabilities. The geometric coefficients in the basic equations differ significantly from simple toroidicity, and do not, in general, allow to apply results found in tokamak geometry to a stellarator. For example, it has been demonstrated that the turbulent transport by drift-Alfvén waves is affected by the local magnetic shear.[1] In this work, we want to study some aspects of electron temperature gradient (ETG) turbulence in stellarator geometry, exploring differences and similarities with respect to the tokamak case.

Electron heat transport in present-day stellarators is often dominated by neoclassical processes.[2] On the other hand, it is observed that turbulent contributions with a gyro-Bohm-type scaling also play a role.[2,3] At this stage, our knowledge about the mechanisms underlying anomalous electron thermal transport in stellarators is quite fragmentary, however. One obvious candidate is the trapped electron mode (TEM), but at least in some cases, it seems to leave the global confinement unaffected.[2] Moreover, attempts to reduce the neoclassical transport in next-generation experiments via magnetic field optimization happens to also weaken the role of TEMs since regions of large magnetic curvature and high trapped particle fraction tend to be separated. So the question naturally arises if there are other microinstabilities potentially causing electron thermal transport.

Nonlinear gyrokinetic simulations of tokamak plasmas have shown that ETG turbulence at hyperfine scales (see, e.g., Ref. 4, and references therein) may exhibit high-amplitude radial streamers, yielding experimentally relevant electron heat fluxes despite its low intrinsic mixing length level.[4,5] If this surprising finding also holds for stellarators, ETG modes should be considered as a possible source of electron heat transport. Tokamak simulations show that the presence or absence of ETG streamers is dependent on details of the magnetic geometry, namely the value of the global magnetic shear, $\hat{s}$, and the normalized pressure gradient, α.[4] Therefore it is not *a priori* clear if one should expect ETG transport to be relevant for stellarators or not. Direct numerical simulations will have to provide the answer. Besides this question, we will also address the (co-)existence, nature, and role of turbulence-driven zonal flows and fields on hyperfine scales. These purely radial variations of the perturbed electromagnetic potentials $\tilde{\phi}$ and $\tilde{A}_{\parallel}$ are associated with $\mathbf{E}\times\mathbf{B}$ flows and magnetic field fluctuations. They can be self-generated by the turbulence and may in turn act as its dominant nonlinear saturation mechanism.[6–12]

In the absence of generic model magnetohydrodynamic equilibria for stellarators, we will focus specifically on Wendelstein 7-AS,[13] which can be seen as a prototype for a certain important class of magnetic fusion devices called ''helical advanced stellarators.'' Our nominal physical parameters are based on the Wendelstein 7-AS discharge No. 49689 at an effective minor radius of 6 cm, i.e., at about 1/3 of the effective minor radius of the last closed flux surface. The electron density and temperature are given by $n_e = 2.2\cdot 10^{19}\ \mathrm{m}^{-3}$ and $T_e = 2.3$ keV, respectively, their normalized gradients are $R/L_{n_e} = -(R/n_e)(dn_e/dr) = 0$ and $R/L_{T_e} = -(R/T_e)(dT_e/dr) = 10$, where $R = 2.0$ m is the ma-

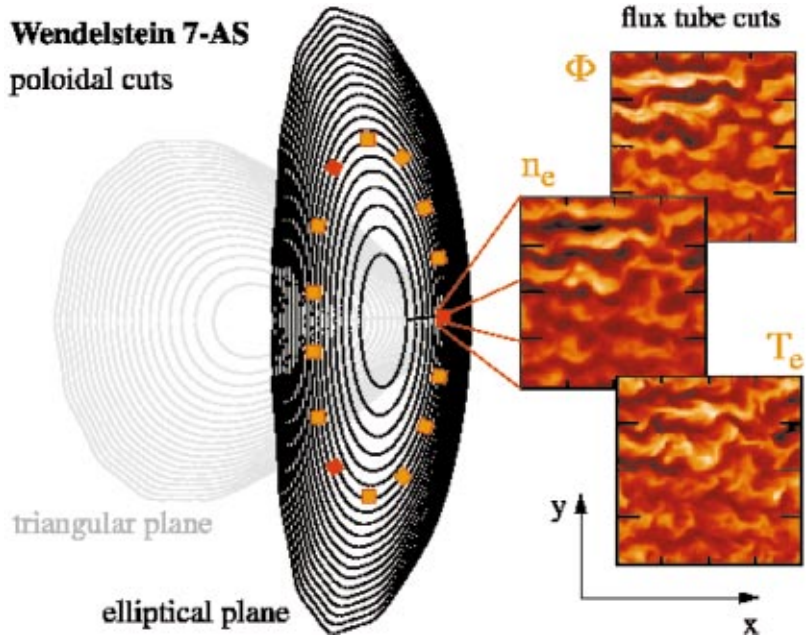

FIG. 1. (Color) Poloidal cross sections of Wendelstein 7-AS together with representative flux tubes. The turbulence exhibits high-amplitude radial streamers.

jor plasma radius. The magnetic field strength is $B=2.5$ T, the rotational transform is $\iota=1/q\approx 1/3$, and the global magnetic shear is $\hat{s}=-(r/\iota)(d\iota/dr)\approx 0$. The nominal value for $\tau=Z_{\mathrm{eff}}(T_e/T_i)$ was chosen to be unity, and the electron plasma beta is given by $\beta_e=8\pi n_e T_e/B^2=0.32\%$. From a critical gradient formula for ETG modes in Wendelstein W7-AS,[14] it can be inferred that the nominal $R/L_{T_e}=10$ is clearly above $(R/L_{T_e})_{\mathrm{crit}}\approx 2.5$.

We now turn to some fundamental aspects of nonlinear gyrokinetic computations of turbulence and transport in Wendelstein 7-AS. The fact that we deal with perpendicular scales of the order of only a few ion gyroradii in a configuration with $\iota\approx 1/3$ and $\hat{s}\approx 0$ means that it is justified to employ the well-established method of flux-tube simulations,[15] using periodic boundary conditions in the field-line following coordinate after three toroidal turns and neglecting perpendicular variations of the geometric coefficients. This is a significant simplification compared to global simulations which may be needed in some cases, particularly for larger scale turbulence in smaller devices.[16,17] Note that despite the broken continuous axisymmetry, there remains a fivefold discrete symmetry which ensures that a fair proportion of the flux surface is already sampled by only one representative flux tube. The situation is visualized in Fig. 1 by means of a Poincaré plot.

For our nonlinear simulations, we choose a flux tube (shown in red) which intersects the outboard side of the elliptical plane because, for the nominal physical parameters given above, it exhibits the largest linear growth rates. Shown in orange are the other four equivalent flux tubes. The geometric input data that specifies the three-dimensional magnetic field structure is generated by means of the Gourdon code[18] as a Fourier expansion in straight-field-line coordinates. The nonlinear electromagnetic gyrokinetic Vlasov-Maxwell equations[19,20] are solved on a fixed grid in five-dimensional phase space by means of a massively parallel code, gene (see Ref. 4). The simulations are carried out in a magnetic flux tube with perpendicular dimensions of $128\,\rho_e$, where ρ_e is the gyroradius of thermal electrons. The ions are taken to respond adiabatically, and trapped electron effects are neglected. We use 64 grid points in all three spatial directions, and 30×10 points in $(v_\parallel,\mu)$ space.

Because of the low intrinsic mixing length level for ETG modes, the presence of high-amplitude streamers is vital in order to achieve experimentally relevant values of the electron heat conductivity χ_e.[4,5] Here, we present simulations of ETG turbulence in stellarator geometry for the above nominal parameters, investigating this issue. As can be seen from snapshots of $\tilde{\phi}$, $\tilde{n}_e$, and $\tilde{T}_e$ in Fig. 1 for the fully developed turbulence, the system indeed exhibits high-amplitude $[(e\tilde{\phi}/T_{e0})(L_{T_e}/\rho_e)\sim 10]$ radially elongated vortices. In physical units, $e\tilde{\phi}/T_{e0}\sim\tilde{n}_e/n_{e0}\sim 0.2\%$ and $\tilde{T}_e/T_{e0}\sim 0.25\%$ which significantly exceeds the mixing length expectations, $e\tilde{\phi}/T_{e0}\sim\tilde{n}_e/n_{e0}\sim\tilde{T}_e/T_{e0}\sim\rho_e/L_{T_e}\sim 0.023\%$. On the other hand, the average streamer aspect ratio computed from the FWHM values of the radial and poloidal autocorrelation functions of $\tilde{\phi}$ [see Fig. 2(a)] is given by $\Delta_x/\Delta_y=21\rho_e/10.5\rho_e=2.0$. Obviously, ETG transport levels way beyond the mixing length estimate are due to both finite vortex aspect ratios *and* enhanced fluctuation amplitudes.

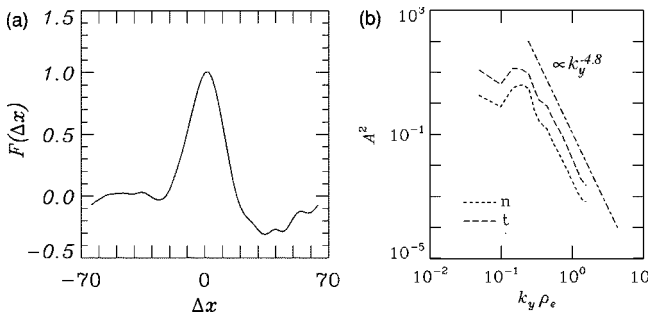

FIG. 2. Radial autocorrelation function of $\tilde{\phi}$ as a function of Δx in units of ρ_e, and k_y spectra of $\tilde{n}_e^2$ and $\tilde{T}_e^2$, denoted, respectively, by n and t.

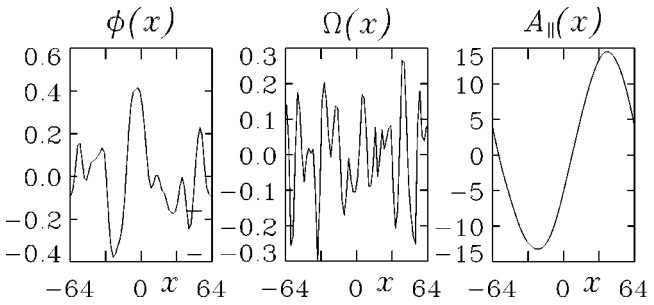

FIG. 3. Snapshot of flux surface averaged values of $\tilde{\phi}$, $\tilde{\Omega}\equiv\tilde{v}'_{Ey}$, and $\tilde{A}_\parallel$ as a function of the radial coordinate x.

Moreover, the induced transport of $\chi_e \sim 12\rho_e^2 v_{te}/L_{T_e}$ is clearly dominated by its electrostatic part (associated with perpendicular $\mathbf{E}\times\mathbf{B}$ advection), with the electromagnetic component (due to fast electron motion along perturbed magnetic field lines) contributing only some 2% to the total χ_e. This finding is consistent with earlier tokamak results and has been discussed in Ref. 21.

Hence we have demonstrated that the occurrence and dominance of high-amplitude ETG streamers is, in general, not dependent on a particular kind of magnetic geometry (i.e., that of a tokamak). Here, we would like to stress once again that given the $\hat{s}$-α dependence in the tokamak case (see Ref. 4), this result is by no means trivial. In particular, for a tokamak with no significant global magnetic shear, one would *not* observe streamers. As is shown in Ref. 22, the ETG transport levels are generally explained well by a model which simply balances the linear growth rates, γ_L, of long-wavelength streamers with the growth rates of secondary instabilities, γ_S (see also Ref. 5). Among the latter are Kelvin–Helmholtz-type modes driven by gradients of the perpendicular and parallel velocity gradients of the primary instabilities. Since γ_S is proportional to the amplitude of the primary, the saturation amplitude follows from $\gamma_S \sim \gamma_L$. It is hard if not impossible to predict the outcome of this interplay in a magnetic geometry as complex as the one under investigation here.

In Fig. 2(b), the k_y spectra of two quantities are presented: $\tilde{n}_e^2$ and $\tilde{T}_e^2$, denoted, respectively, by n and t. Both spectra have pronounced peaks around $k_y\rho_e \sim 0.2$ (despite the fact that the linearly most unstable modes have $k_y\rho_e \sim 0.4$) and display a strong drop for $k_y\rho_e \gtrsim 0.3$ which can be approximately described by a power law, $A \propto k_y^{-2.4}$. It is interesting to note that almost the same exponent has been found in tokamak simulations of both ETG and drift-wave turbulence as described, respectively, in Refs. 22 and 23. This agreement of the scaling exponents is not surprising, however, given the fact that the role of the perpendicular $\mathbf{E}\times\mathbf{B}$ nonlinearity controlling the cascade dynamics is the same in all three cases. The central importance of long-wavelength ETG modes in the turbulent system has an interesting implication: Repeating the above simulation, taking into account finite electron Debye length effects ($\lambda_{De}/\rho_e = 1.7$ for our nominal parameters), χ_e is only reduced by a factor of 2 (reflecting the change of the linear growth rates at $k_y\rho_e \lesssim 0.2$), despite the fact that all modes with $k_y\rho_e \gtrsim 0.4$ are linearly stabilized. The nonlinear k_y spectra are found to be very similar to the ones displayed in Fig. 2(b), except that they tend to peak at slightly lower values of k_y.

Having established the existence of high-amplitude streamers, and having studied some of their main properties, we would now like to address the following question: How important are zonal flows and fields, i.e., purely radial ($k_y = k_\parallel = 0$) fluctuations of $\tilde{\phi}$ and $\tilde{A}_\parallel$? Both of these components of the turbulent system are generated nonlinearly and can decorrelate the turbulent eddies that drive them. Zonal flows and fields lead to radial variations of the poloidal $\mathbf{E}\times\mathbf{B}$ flow and magnetic shear, respectively, keeping the average deviation at zero at all times. A typical snapshot of the flux-surface averaged values of $\tilde{\phi}$ and $\tilde{A}_\parallel$ (in normalized units) as a function of the radial coordinate x (normalized to ρ_e) is plotted in Fig. 3. From data like this, one can compute the radial profiles of both the $\mathbf{E}\times\mathbf{B}$ shearing rate, $\tilde{\Omega}\equiv\tilde{v}'_{Ey}$, and the magnetic shear fluctuation, $\tilde{s}\equiv qR\tilde{B}'_y/B$, where the prime stands for d/dx. The space and time averaged RMS values are given by $\tilde{\Omega}^{\rm rms} \approx 0.12\, v_{te}/R \sim 0.3\, \gamma^{\max}$ and $\tilde{s}^{\rm rms} \approx 0.018$, where $\gamma^{\max}$ is the maximum linear growth rate. ($\tilde{\Omega}$ can reach local and instantaneous peak values which are about three times larger than that as can be seen in Fig. 3 where $\tilde{\Omega}$ is shown in units of v_{te}/R.) This is in contrast to results from ITG turbulence where $\tilde{\Omega}$ can significantly exceed $\gamma^{\max}$ (e.g., $\tilde{\Omega}^{\max}/\gamma^{\max} \sim 14$ in Ref. 24). In the latter case, one obtains the zonal flow saturation criterion $\tilde{\Omega}^{\rm rms} \sim \gamma^{\max}$ only after correcting for the ineffectiveness of the high frequency component of $\tilde{\Omega}$. Moreover, the zonal components of ETG turbulence contribute only 1% or so to the total $\tilde{\phi}^{\rm rms}$. This is again in contrast to the findings in the ITG case where zonal modes with $k_x\rho_i \sim 0.1$ tend to contribute significantly or even dominate the fluctuation free energy contained in $\tilde{\phi}$ (see, e.g., Ref. 24, and references therein).

It is well known that low-amplitude ITG streamers are broken up by zonal flows.[9,10] In the ETG case, however, the self-generated zonal flows are too weak (about 15–20 times weaker than in the ITG case as we have shown above) to break up the high-amplitude streamers as is obvious from Fig. 1. Moreover, since magnetic shear variations primarily affect the linear growth rates of the ETG modes driving the turbulence,[12] a value of $\tilde{s}^{\rm rms} \approx 0.018$ is certainly too small for zonal fields to play a significant role. Similar zonal flow/field saturation levels as the ones reported here have also been found in ETG simulations of tokamak plasmas. Thus, we may conclude that, at least for a significant region in parameter space, zonal modes on electron gyroradius scales behave more or less passively. A notable exception could be the ETG simulations for tokamak edge parameters described in Ref. 21.

Nevertheless, it is still of interest to study the spectral properties of zonal flows and fields, e.g., in order to allow for comparisons with analytic theories of nonlinear zonal mode generation and saturation. The k_x spectra of these zonal fluctuations are plotted in Figs. 4(a) and 4(b). Whereas zonal $\tilde{\phi}$'s are excited over a wide range of k_x values ($0.1 \lesssim k_x\rho_e \lesssim 1$), zonal $\tilde{A}_\parallel$'s tend to be dominated by the lowest (finite) k_x

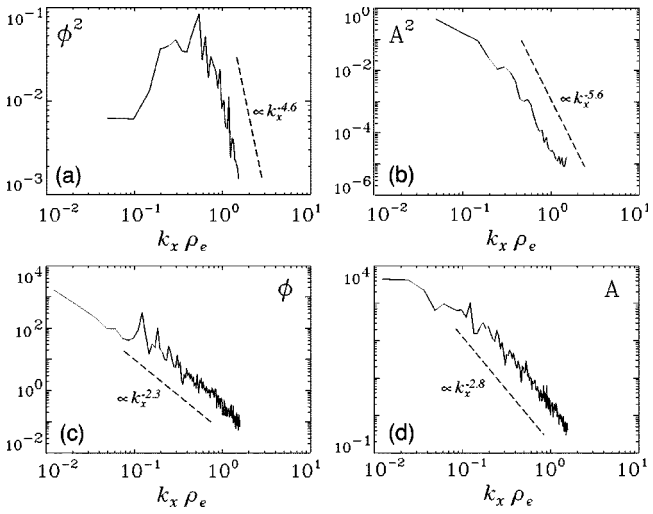

FIG. 4. Time-averaged k_x spectra of the flux surface averaged values of $\tilde{\phi}$ and $\tilde{A}_\parallel$ (zonal flows and fields) [(a),(b)]. A tokamak case is shown for comparison [(c),(d)].

mode (see also Fig. 3). The drop of the zonal component of $\tilde{\phi}$ at low k_x may be understood in terms of a reduction by k_x^2 relative to the ITG case (both a secondary instability analysis[5] and inspection of the gyrokinetic Poisson equation[4] show that) which in turn exhibits a $1/k_x$ behavior at low k_x.[24] For $k_x \rho_e \gtrsim 0.5$, the spectra exhibit a power law decay, $\tilde{\phi} \propto k_x^{-\nu}$ and $\tilde{A}_\parallel \propto k_x^{-\mu}$, where $\nu = 2.3 \pm 0.3$ and $\mu = 2.8 \pm 0.3$. Changing the value of β_e to half its nominal value yields the same exponents. It is interesting to note that the turbulent k_y spectrum [see Fig. 2(b)] and the zonal k_x spectrum of $\tilde{\phi} \propto \tilde{n}_e$ fall off with similar exponents. This suggests that the same turbulent cascade processes might determine the exponents of both types of spectra. If this were true, we would expect these exponents to be quite universal because the role of the perpendicular nonlinearities is invariant under geometric changes. To test this idea, we simulated a tokamak plasma with $R/L_n = 2.2$, $R/L_{T_e} = R/L_{T_i} = 6.9$, $q = 1.4$, $\hat{s} = 0.8$, $\tau = 1$, $m_i/m_e = 100$, and $\beta_e = 10^{-3}$. The perpendicular box size was 512 ρ_e with 2 ρ_e per grid cell, and the adiabatic ion approximation was dropped. The resulting k_x spectra of zonal flows and fields are shown in Figs. 4(c) and 4(d). (Other aspects of these two-species, two-scale ITG-ETG simulations will be presented elsewhere.) Figure 4(c) shows that the drop of the zonal flow spectrum at low k_x observed in Fig. 4(a) is due to ion adiabaticity and the absence of longer-wavelength turbulence. Furthermore, for this completely different system, we basically get the same exponents over a wider range in k_x space. Such robustness indicates that a generic theory based on cascade dynamics might be able to capture the essence of the underlying mechanism(s).

In summary, we have presented the first simulations of stellarator core turbulence, examining some key characteristics of gyrokinetic ETG turbulence in the geometry of Wendelstein 7-AS. We find that high-amplitude ETG streamers may also appear in a magnetic geometry other than that of a tokamak, raising χ_e to experimentally relevant values. Given the $\hat{s}$-α dependence in the tokamak case, this result is by no means trivial. In particular, for a tokamak with no significant global magnetic shear, one would *not* observe streamers. ETG turbulence should therefore be considered as a possible source of electron heat transport in stellarators. Zonal flows and fields tend to play a subdominant role in the turbulent dynamics, at least for a significant region in parameter space. Many of the spectral properties of zonal modes are observed to be quite universal, indicating that a generic theory of zonal modes at hyperfine scales might be constructable on the basis of cascade physics.

ACKNOWLEDGMENTS

We would like to thank W. Dorland, G. W. Hammett, P. H. Diamond, C. Holland, M. Endler, and E. Holzhauer for stimulating discussions. The computations were performed at the Leibniz Computing Center and at the Garching Computing Center.

[1] A. Kendl, Plasma Phys. Controlled Fusion **42**, L23 (2000).
[2] H. Maassberg, R. Brakel, R. Burhenn *et al.*, Plasma Phys. Controlled Fusion **35**, B319 (1993).
[3] F. Wagner and U. Stroth, Plasma Phys. Controlled Fusion **35**, 1321 (1993).
[4] F. Jenko, W. Dorland, M. Kotschenreuther, and B. N. Rogers, Phys. Plasmas **7**, 1904 (2000).
[5] W. Dorland, F. Jenko, M. Kotschenreuther, and B. N. Rogers, Phys. Rev. Lett. **85**, 5579 (2000).
[6] A. Hasegawa and M. Wakatani, Phys. Rev. Lett. **59**, 1581 (1987).
[7] B. A. Carreras, V. E. Lynch, and L. Garcia, Phys. Fluids B **3**, 1438 (1991).
[8] P. H. Diamond and Y. B. Kim, Phys. Fluids B **3**, 1626 (1991).
[9] G. W. Hammett, M. A. Beer, W. Dorland, S. C. Cowley, and S. A. Smith, Plasma Phys. Controlled Fusion **35**, 973 (1993).
[10] B. I. Cohen, T. J. Williams, A. M. Dimits, and J. A. Byers, Phys. Fluids B **5**, 2967 (1993).
[11] P. N. Guzdar, R. G. Kleva, A. Das, and P. K. Kaw, Phys. Rev. Lett. **87**, 015001 (2001).
[12] C. Holland and P. H. Diamond, Phys. Plasmas **9**, 3857 (2002).
[13] H. Renner, Plasma Phys. Controlled Fusion **31**, 1579 (1989).
[14] F. Jenko and A. Kendl, New J. Phys. **4**, 35 (2002).
[15] M. A. Beer, S. C. Cowley, and G. W. Hammett, Phys. Plasmas **2**, 2687 (1995).
[16] G. Jost, T. M. Tran, W. A. Cooper, L. Villard, and K. Appert, Phys. Plasmas **8**, 3321 (2001).
[17] R. E. Waltz, J. M. Candy, and M. N. Rosenbluth, Phys. Plasmas **9**, 1938 (2002).
[18] C. Gourdon, D. Marty, E. Maschke, and J. Dumont, in *Proceedings of the 3rd International Conference on Plasma Physics*, Novosibirsk, 1968, edited by IAEA (IAEA, Vienna, 1969), Vol. 1, p. 847.
[19] T. Antonsen and B. Lane, Phys. Fluids **23**, 1205 (1980).
[20] E. A. Frieman and L. Chen, Phys. Fluids **25**, 502 (1982).
[21] F. Jenko and W. Dorland, Plasma Phys. Controlled Fusion **43**, A141 (2001).
[22] F. Jenko and W. Dorland, "Prediction of significant tokamak turbulence at electron gyroradius scales," Phys. Rev. Lett. (submitted).
[23] S. J. Camargo, D. Biskamp, and B. Scott, Phys. Plasmas **2**, 48 (1995).
[24] T. S. Hahm, M. A. Beer, Z. Lin *et al.*, Phys. Plasmas **6**, 922 (1999).